

<http://ansinet.com/itj>

ITJ

ISSN 1812-5638

# INFORMATION TECHNOLOGY JOURNAL

**ANSI***net*

Asian Network for Scientific Information  
308 Lasani Town, Sargodha Road, Faisalabad - Pakistan

## 3D Medical Image Segmentation and Surface Modeling Using the Power Crust

K. Kies, N. Benamrane and A. Benyettou

Département d'Informatique, S.I.M.P.A, U.S.T.O BP1505 El Mnaouer Oran 31000 (Algeria)

---

**Abstract:** we present a method of 3D segmentation based on region-growing technique were extracted region surface edges are modelled using a 3D Delaunay Triangulation refined by using the power crust algorithm. The latest can be performed either on a small subset randomly chosen or on all edge points. This proposed fast and very promising approach makes it possible to adapt it to the segmentation of anatomical structures in MRI and CTScan images.

**Key words:** Medical images, 3D segmentation, region growing, delaunay triangulation

---

### INTRODUCTION

Automatic 3D image segmentation is an indispensable tool and remains a major problem for image analysis. Proposed approaches attempting to solve the 3D segmentation problem are numerous and extremely varied. The choice of a method depends on the nature of the image, what predicates are to be extracted and what are the usage constraints (algorithm complexity, real time requirement, memory available, etc.). Region growing have received considerable attention from 2D an 3D image analysts and researchers. The principle of the technique is to define some criteria, called homogeneity criteria, which allow regrouping connected image pixels into larger regions. These criteria are often based on differential surface characteristics of the 3D object and a stable segmentation in quadric pieces is achieved<sup>[1]</sup>. They can also be obtained from some evaluation function<sup>[2]</sup> or by RMS-approximation of image points by simple polynomial surfaces (plane or quadric)<sup>[3]</sup>. Region growing method has also been used for 3D medical image reconstruction where the voxel gray level defines some density of the volume to reconstruct as well as a regrouping criteria.

Deformable models have also been successful in the field of vision and image analysis<sup>[4]</sup>. They allow segmentation and object reconstruction by providing compact geometric representations where evolutions laws similar to physical mechanics laws are introduced (forces, physical constraints and friction)<sup>[5-6]</sup>. Procedures using deformable models have been widely used for

3D segmentation since they are well suited for object extraction from temporal and volumetric data from image sequences such as IRM, CT scanned, X Tomography, ARM and Echography<sup>[9-11]</sup>. These procedures have been more efficient by using 3D Pyramid images<sup>[12]</sup> and such hierarchical structures allow coarse to fine type segmentation. Region and edge information has been integrated into these models making them more efficient<sup>[13]</sup>.

Another approach that is fundamentally geometrical: mathematical morphology, which mainly consists on comparing objects under analysis to another object with known shape. Morphologic operators applied to 3D images are described<sup>[14]</sup> where, temporal image sequences considered as 3D images are segmented. Three-dimensional segmentation, based on mathematical morphology, has been applied to anatomical structures in MR images on large databases<sup>[15]</sup>.

The so called Biologists methods (neural networks, genetic algorithms, etc.) have also been extensively used for 3D image analysis and especially segmentation<sup>[16,17]</sup>. In quest of better efficiency and precision various hybridations of different techniques have been successfully attempted<sup>[18-24]</sup>.

### THE PROPOSED APPROACH

In this study we propose a method for 3D Image segmentation based on region growing, followed by 3D Delaunay triangulation as a first step in order to extract

and model the crust of the obtained 3D regions using. The power crust theorem is used to obtain the final segmentation. The essential steps are described in the following:

**Region growing:** In this step, we propose to perform simultaneous 2D segmentation for each slice following the hierarchical region growing algorithm proposed in<sup>[25]</sup>. The regrouping strategy is based on three criteria applied hierarchically to regroup adjacent pixels that are sufficiently similar. These criteria are:

- Gray levels amplitude variation,
- Variance of gray levels for more or less uniform regions,
- Gradient norm per unit frontier length across adjacent regions.

The uniformity predicates associated to the characteristic attributes of region say  $R_i$  are as follow:

- $P_1(R_i) = [(MAX_i - MIN_i) < Threshold_1]$  where,  $MAX_i$  and  $MIN_i$  are respectively the minimum and maximum gray level in region  $R_i$
- $P_2(R_i) = [V(R_i) < Threshold_2]$  where,  $V(R_i)$  is the gray level variance of points in region  $R_i$ . we have  $Threshold_2 = (Threshold_1)^2$
- $P_3(R_i) = [(a_2/a_1) < Threshold_3]$  where,  $a_1$  is the frontier length between two adjacent regions and  $a_2$  is the cumulated gradient norm along the frontier.

After using these criteria, we obtain a set of regions each characterized by the contour points and by attributes such as: surface (volume), perimeter (surface area), average gray level, variance, etc.

**Identifying and linking regions:** In this second step, segmentation results from two adjacent slices are fused in the following manner: we start from a region of interest  $R_L$  in slice  $L$ , all set of points  $P_L(x,y)$  (having  $(x,y)$  coordinates in slice  $L$ ) of region  $R_L$  are labeled with same index region corresponding to the set of attributes determined in previous step. Starting from a point  $P_L(x,y) \in R_L$ , we examine its homologue  $P_{L+1}(x,y)$  with the same  $(x,y)$  coordinates on slice  $L+1$ , if these two points are similar with respect to criteria defined previously, then there region indexes are identified, otherwise try all other  $P_L(x,y)$ . If none of them are similar, this simply means region  $R_L$  ended in slice  $L$  and a new region started at next slice  $L+1$  and therefore

retains its index. This process is done for all regions in slice  $L$  and then we move on onto next slice  $L+1$  until last slice.

**3D surface reconstruction:** Once done with previous steps, each region of the segmented 3D image is a closed surface (called the crust) defined by its surface edge points. In practice, even for modest regions, the number of points can be quite big (for example a 20 pixel diameter cylinder across 10 slices count some 600 points) while large regions may count more than 100 000 points. Since we intend to use 3D Delaunay triangulation (3DT), we may face the problem that most existing implementations are slow, or at least too slow to be considered. Fortunately, this is not the case and there are many good routines available free of charge<sup>[26-29]</sup>. The outcome of 3DT is a set of pair wise linked edge points, in which each link triplet forms a triangular face and each face quadruplet forms a tetrahedron. The crust of the region of interest is a subset of the set of all triangular faces resulting from 3DT. If the crust is convex that the solution is straightforward: it is the Convex Hull<sup>[26]</sup>. To tackle the problem of the Concave Hull, very elaborated algorithms have been developed.

In this study we used principally Nina Amanta's Powercrust<sup>[28]</sup>. We have also Patrice Koehl's very nice program Tetrafor<sup>[29]</sup>, which has very efficient 3D Delaunay Triangulation (Weighted). Once the crust faces obtained, there is one final twist which consists on correctly orienting the normal of each face toward the outside of the object. The success of this last step allows for a 3D rendering with no defects during final visualization of the results.

## RESULTS

In order to validate present results, we have tested this method on various test 3D images containing various simple objects (cubes, spheres and cylinders). We have segmented a 109 slices 256x256 16bit MRI Brain 3D image and extracted and reconstructed the outer crust. Figure 1 shows one slice (negative gray scale) and below, its corresponding edges of interest.

On Fig. 2, the set of all edges obtained using procedure described in previous section for the region of interest is shown (here the entire head).

The 3D rendering after using one tenth off all edge points as input for powercrust is shown on Fig. 3. More details are obtained when using all the edge points (Fig. 4).

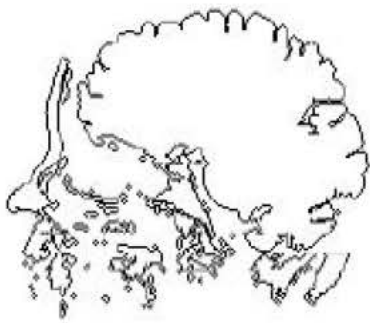
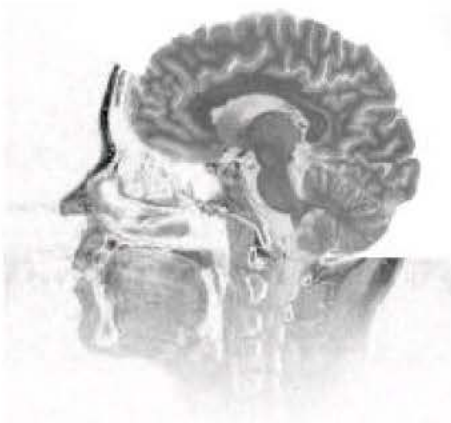


Fig. 1: One segmented slice and edges of interest

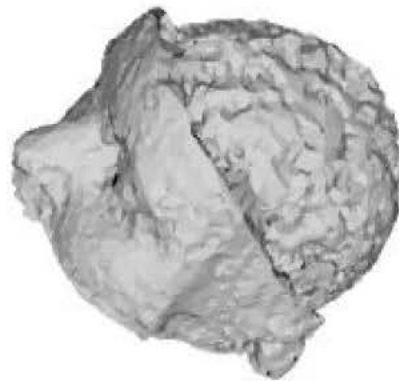


Fig. 3: Ten percent of contour points randomly chosen (5000 points)



Fig. 4: All contour points used (100000 points)

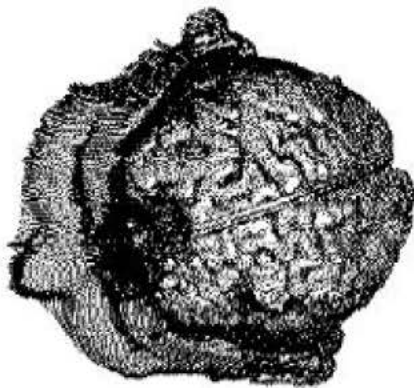


Fig. 2: Set of all edges

Similar results were obtained from CT Scanner images, for instance, Fig. 5 shows the skull of a Monkey reconstructed from a set of 256 slices.

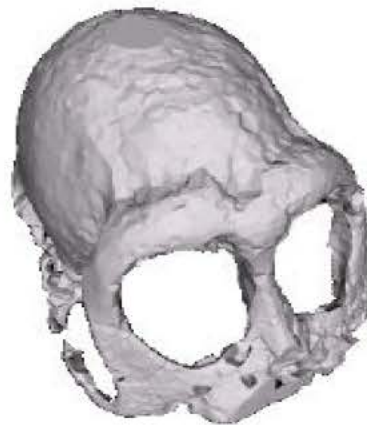


Fig. 5: Skull of a Monkey

## CONCLUSIONS

We presented a method of 3D segmentation and applied it to some test images. A region-growing technique followed by a surface modelling using Powercrust is done. The generality of the proposed approach makes it possible to adapt it to the segmentation of anatomical structures in medical images. Tissue such as skin, muscles, eyes, etc.. can be extracted and modelled since the segmentation of all these tissue is crucial for the construction of a complete realistic models.

An ongoing work is underway to implement this method on a PC cluster where better performance is expected.

## REFERENCES

1. Monga, O. and I. Bricault, 1994. From volume medical images to quadric surface patches. R.R. n°2380. Inria.
2. Revol, C. and M. Jourlin, 1997. A new minimum variance region growing algorithm for image segmentation. *Pattern Recognition Lett.*, 18: 249-258.
3. Mourad, D., 1998. Segmentation des Images de profondeurs utilisant les analyses multi-resolutions. Thèse LIGIM.
4. Kaas, M. A. Itkin and D. Terzopoulos, 1998. Snakes: Active contour models. *Intl. J. Computer Vision*, 1: 312-331.
5. Jaques, O., 1998. Lachaud Extraction de surfaces à partir d'images tridimensionnelles : approche discrète par modèle déformable. Ph.D Thesis, Université de Joseph Fourier.
6. Lachaud, J.O. and A. Montavert, 1998. Deformable meshes with automated topology changes for coarse to fine dimensional surface extraction. *Medical Image Analysis*, pp: 187-207
7. Nicola, S., 2000. Optimisation topologique et géométrique d'un maillage surfacique dynamique: Application à la segmentation des images médicales volumiques. Rapport de recherche Inria Sophia-Antipolis, Projet Epidaure
8. Montagnat, J., H. Delingette and N. Ayache. 2001. A review of deformable surfaces: Topology, geometry and deformation. *Image and Vision Computing*, 19: 1023-1040.
9. Isaac, C., 1992. Modèles déformables 2D et 3D: application à la segmentation d'images médicales. Ph.D Thesis, Université de Paris IX Dauphine.
10. Johan, M., 1999. Modèles déformables pour la segmentation et modélisation d'images médicaux 3D et 4D. Ph.D Thesis, Nice Sophia-Antipolis.
11. Hervé, D. and M. Johan, 1999. Extension des maillages simplexes pour la segmentation d'images 3D et 4D *Projet Epidaure*.
12. Jaques, O., 1999. Lachaud Extraction de formes et segmentation d'images volu-métriques par modèle déformable.
13. Pardo, X.M., M.J. Carreira, A. Mosquera and D. Cabello, 2001. A snake for CT image segmentation integrating region and edge deformation. *Image and Vision Computing*, 19: 461-475.
14. Agnus, A., C. Ronse, F. Heitz, 2000. Segmentation spatio temporelle morpho-logique de séquences d'images. LSIIT. UPRES-A 7005, Université de Strasbourg.
15. Bueno, G., O. Musse, F. Heitz, J.P. Armspash, 2000. Three-dimensional analysis of anatomical structures in MR images on large databases. Université Louis Pasteur (Strasbourg I). LSIIT. CNRS-UPRES- A7005.
16. Takatsuka, M. and R.A Jaivis, 2001. Encoding 3D structural Information using multiple self-organizing feature maps. *Image and Vision Computing*, 19: 99-118.
17. Kobashi, S., Y. Hata, F. Miyawaki and N. Kaniura, 2001. Volume-quantization-based neural network approach to 3D MR angiography's image segmentation. *Image and Vision Computing*, 19: 185-193.
18. Eun, Y.K., W.H. Sang, P. Se Hyun and J.K. Hang, 2001. Spatiotemporal segmentation using genetic algorithms *Pattern Recognition*, 34: 2063-2066.
19. Benoit-Cattin, H., T. Zouagi and C. Odet, 2001. Une vision fonctionnelle de la segmentation d'images. *Creatis, Unité de Recherches CNRS (UMR5515)*.
20. Thierry, G., 1998. Segmentation automatique des structures cérébrales internes en imagerie par résonance magnétique tridimensionnelle. Ph.D Thesis, Université de l'ENST Paris.
21. Marc, G., 1998. Segmentation spatio-temporelle et suivi dans une séquence d'images: Application à la structuration et à l'indexation vidéo. Ph.D Thesis, Université de RENNES I.
22. Tina, K., W. Eric, L. Grimson and M. William, 1996. Wells and Ron Kikinis. Segmentation of brain tissue from magnetic resonance images. *Medical Image Analysis*, 1: 109-127.
23. Baillard, P.H. and C. Barillot, 2001. Segmentation of brain 3D images using level sets and dense registration. *Medical Image Analysis*, 5: 185-194.
24. Rey, D., G. Subsol, H. Delingette and N. Ayache, 2002. Automatic detection and segmentation of evolving processes in 3D images: Application to multiple sclerosis. *Medical Image Analysis*, 6: 163-179.

25. Horand et, R., O. Monga, 1993. *Vision Par Ordinateur*. Edn Hermes, Paris.
26. Qhull, Version 2.6 April 19, 1999, Convex hull, Delaunay triangulation, Voronoi diagrams, Halfspace intersection. <http://www.geom.umn.edu/locate/qhull>.
27. CGAL, Computational Geometry Algorithms Library. Copyright(c), 1997-2002. The CGAL Consortium. <http://www.cgal.org>
28. Nina, A., C. Sunghee and K.K. Ravi, 2000. Powercrust, Power Crust software, Copyright (C) by the University of Texas.
29. Tetrafor, 1996. A 3D weighted Delaunay Triangulation Copyright (C) 2002 Patrice Koehl [koehl@csb.stanford.edu](mailto:koehl@csb.stanford.edu). H. Edelsbrunner and N.R. Shah, *Algorithmica*, 15: 223-241.